0022-3565/10/3341-147–155$20.00
THE JOURNAL OF PHARMACOLOGY AND EXPERIMENTAL THERAPEUTICS
JPET 334:147–155, 2010
Copyright © 2010 by The American Society for Pharmacology and Experimental Therapeutics
Vol. 334, No. 1
167601/3602208
Printed in U.S.A.

Distribution of Gefitinib to the Brain Is Limited by P-glycoprotein (ABCB1) and Breast Cancer Resistance Protein (ABCG2)-Mediated Active Efflux

Sagar Agarwal, Ramola Sane, Jose L. Gallardo, John R. Ohlfest, and William F. Elmquist

Department of Pharmaceutics (S.A., R.S., W.F.E.), Department of Pediatrics (J.L.G., J.R.O.), Department of Neurosurgery (J.R.O.), University of Minnesota, Minneapolis, Minnesota; and Brain Barriers Research Center, University of Minnesota, Minnesota (W.F.E., J.R.O.)

Received February 23, 2010; accepted April 23, 2010

ABSTRACT

Gefitinib is an orally active inhibitor of the epidermal growth factor receptor approved for use in patients with locally advanced or metastatic non–small cell lung cancer. It has also been evaluated in several clinical trials for treatment of brain tumors such as high-grade glioma. In this study, we investigated the influence of P-glycoprotein (P-gp) and breast cancer resistance protein (BCRP) on distribution of gefitinib to the central nervous system. In vitro studies conducted in Madin-Darby canine kidney II cells indicate that both P-gp and BCRP effectively transport gefitinib, limiting its intracellular accumulation. In vivo studies demonstrated that transport of gefitinib across the blood-brain barrier (BBB) is significantly limited. Steady-state brain-to-plasma (B/P) concentration ratios were 70-fold higher in the *Mdr1a/b(−/−) Bcrp1(−/−)* mice (ratio of approximately 7) compared with wild-type mice (ratio of approximately 0.1). The B/P ratio after oral administration increased significantly when gefitinib was coadministered with the dual P-gp and BCRP inhibitor elacridar. We investigated the integrity of tight junctions in the *Mdr1a/b(−/−) Bcrp1(−/−)* mice and found no difference in the brain inulin and sucrose space between the wild-type and *Mdr1a/b(−/−) Bcrp1(−/−)* mice. This suggested that the dramatic enhancement in the brain distribution of gefitinib is not due to a leakier BBB in these mice. These results show that brain distribution of gefitinib is restricted due to active efflux by P-gp and BCRP. This finding is of clinical significance for therapy in brain tumors such as glioma, where concurrent administration of a dual inhibitor such as elacridar can increase delivery and thus enhance efficacy of gefitinib.

Malignant gliomas account for approximately 70% of all new cases of malignant primary brain tumors diagnosed in the United States every year. Glioblastoma multiforme (GBM) is the most common type of glioma, accounting for approximately 60 to 70% of malignant gliomas (Wen and Kesari, 2008; CBTRUS, 2008) and claiming 12,000 lives every year (Davis et al., 2001). Epidermal growth factor receptor (EGFR) and its variant EGFRvIII play a critical role in the development of an aggressive phenotype of GBM; EGFR amplification, mutation, and overexpression are associated with poor prognosis and resistance to therapy (Brandes et al., 2008). Several therapeutic strategies targeting EGFR in GBM have been proposed, including the use of monoclonal antibodies against EGFR or EGFRvIII, vaccine therapies, bispecific antibodies, toxin-linked conjugates, and small molecule tyrosine kinase inhibitors (Omuro et al., 2007).

This work was supported in part by National Institutes of Health National Cancer Institute [Grant CA138437] (to W.F.E. and J.R.O.) and the Children's Cancer Research Fund at the University of Minnesota (to W.F.E, J.R.O). Financial support for S.A. was provided by the Edward G. Rippie Fellowship and the Ronald J. Sawchuk Fellowship in Pharmacokinetics from the Department of Pharmaceutics, University of Minnesota.

Article, publication date, and citation information can be found at http://jpet.aspetjournals.org.

doi:10.1124/jpet.110.167601.

ABBREVIATIONS: CNS, central nervous system; BBB, blood-brain-barrier; MDR1, multi-drug resistance protein 1; P-gp, P-glycoprotein; BCRP, breast cancer resistance protein; A-to-B, apical-to-basolateral; B-to-A, basolateral-to-apical; Peff, effective permeability; B/P, brain-to-plasma; ER, efflux ratio; GBM, glioblastoma multiforme; EGFR, epidermal growth factor receptor; EGFRvIII, epidermal growth factor receptor mutant vIII; *Mdr1*, gene encoding the murine P-glycoprotein; *MDR1*, gene encoding the human P-glycoprotein; *Bcrp1*, gene encoding the murine breast cancer resistance protein; MS, mass spectrometry; ZD1839, gefitinib; ABC, ATP-binding cassette; GF120918 (elacridar), *N*-[4-[2-(6,7-dimethoxy-3,4-dihydro-1*H*-isoquinolin-2-yl)ethyl]-5-methoxy-9-oxo-10*H*-acridine-4-carboxamide]; MDCKII, Madin-Darby canine kidney II; LY335979 (zosuquidar), (*R*)-4-((1a*R*,6*R*,10b*S*)-1,2-difluoro-1,1a,6,10*b*-tetrahydrodibenzo-(*a*,*e*)cyclopropa(*c*)cycloheptan-6-yl)-α-((5-quinoloyloxy) methyl)-1-piperazine ethanol, trihydrochloride; Ko143, (3*S*,6*S*,12a*S*)-1,2,3,4,6,7,12,12*a*-octahydro-9-methoxy-6-(2-methylpropyl)-1,4-dioxopyrazino(1',2':1,6) pyrido(3,4-*b*)indole-3-propanoic acid 1,1-dimethylethyl ester; WT, wild type; DMSO, dimethyl sulfoxide; FVB, Friend Leukemia Virus Strain B.

In recent years, several small molecule inhibitors targeting the tyrosine kinase EGFR have been introduced in clinical practice. Gefitinib (Iressa, ZD1839; AstraZeneca Pharmaceuticals, Macclesfield, Cheshire, UK) is an orally active compound that is a reversible inhibitor of the tyrosine kinase activity associated with EGFR, blocking EGFR signal transduction pathways (Arteaga and Johnson, 2001; Ciardiello and Tortora, 2001; Culy and Faulds, 2002). Despite equivocal results in phase III clinical trials (Giaccone et al., 2004; Herbst et al., 2004), gefitinib was the first drug of its kind to be approved by the United States Food and Drug Administration for monotherapy in patients with locally advanced or metastatic non—small cell lung cancer after failure of at least one prior chemotherapy regimen. However, results from studies evaluating the use of gefitinib for treatment in GBM have been disappointing. In phase II trials of gefitinib, patients with recurrent or progressive high-grade glioma showed no objective response, with a progression-free survival at 6 months of 13 to 14% (Rich et al., 2004; Franceschi et al., 2007). Likewise, no improvement in overall survival was observed in GBM patients at first relapse.

Studies explaining the failure of gefitinib have suggested that the reasons for this lack of efficacy could be related to the heterogeneous molecular characteristics of individual gliomas (Mellinghoff et al., 2005, 2007; Sarkaria et al., 2007) or due to the complexity of signaling pathways, such as negative feedback mechanisms and up-regulation of alternative pathways (Stommel et al., 2007). However, all of these hypotheses are based on a previous assumption that there is adequate delivery of drug to the invasive tumor cells that can be found several centimeters away from the core tumor mass (Kuratsu et al., 1989; Silbergeld and Chicoine, 1997). It is well known that ATP-binding cassette (ABC) transporter proteins, including P-glycoprotein (P-gp/ABCB1) and the breast cancer resistance protein (BCRP/ABCG2), cause multidrug resistance in tumors and actively extrude targeted therapeutics from the brain (Gottesman et al., 2002; Löscher and Potschka, 2005; Fletcher et al., 2010). Certainly, the lack of gefitinib delivery to the invasive tumor cells residing in the CNS behind an intact blood-brain barrier (BBB) is a plausible partial explanation for the lack of efficacy seen in GBM. There have been no published reports that indicate that transport of gefitinib across the intact BBB to the brain is limited. Several groups have studied the interaction of gefitinib with drug transport proteins in vitro and reported contrasting results. Elkind et al. (2005) reported that BCRP actively pumps gefitinib and prevents its tyrosine kinase inhibitor activity. However shortly thereafter, Leggas et al. (2006) reported that gefitinib at clinically relevant concentrations is a potent inhibitor of BCRP and P-gp. Given the lack of evidence to prove that gefitinib can cross the BBB to produce therapeutic concentrations in the brain, it is important to study the brain distribution kinetics of gefitinib and the mechanisms that may influence adequate delivery of gefitinib to the target invasive tumor cells. Here we have used in vitro cell models to demonstrate that gefitinib is a substrate for the ATP transporters P-gp and BCRP. We have also used transporter deficient mice to study the brain distribution of gefitinib. The objective of this study was to establish the interaction of gefitinib with two important transporters of the ABC superfamily, P-gp and BCRP, and to show that distribution of gefitinib across an intact BBB is limited due to active efflux by these two transport proteins.

Materials and Methods

Chemicals and Reagents

[^{14}C]Gefitinib was kindly provided by AstraZeneca Pharmaceuticals. Unlabeled gefitinib and dasatinib were purchased from LC Laboratories (Woburn, MA). [^{14}C]Sucrose and [^{3}H]vinblastine were obtained from Moravek Biochemicals (La Brea, CA). [^{3}H]Prazosin was purchased from PerkinElmer Life and Analytical Sciences (Waltham, MA). [^{14}C]Inulin was purchased from American Radiolabeled Chemicals, Inc. (St. Louis, MO). Elacridar [GF120918, *N*-[4-[2-(6,7-dimethoxy-3,4-dihydro-1*H*-isoquinolin-2-yl)ethyl]-5-methoxy-9-oxo-10*H*-acridine-4-carboxamide]] was purchased from Toronto Research Chemicals Inc. (North York, ON, Canada). Ko143 (Allen et al., 2002) was kindly provided by Dr. Alfred Schinkel (The Netherlands Cancer Institute, Amsterdam, The Netherlands) and zosuquidar [LY335979, (*R*)-4-((1*aR*, 6*R*,10*bS*)-1,2-difluoro-1,1*a*,6,10*b*-tetrahydrodibenzo-(*a*,*e*) cyclopropa(*c*)cycloheptan-6-yl)-α-((5-quinoloyloxy) methyl)-1-piperazine ethanol, trihydrochloride] was a gift from Eli Lilly and Co. (Indianapolis, IN). All other chemicals used were of high-performance liquid chromatography or reagent grade and were obtained from Sigma-Aldrich (St. Louis, MO).

In Vitro Studies

Epithelial Madin-Darby canine kidney (MDCKII) cells were used in all in vitro studies. Wild-type (WT) and MDR1-transfected cells were a gift from Dr. Piet Borst (The Netherlands Cancer Institute). WT and Bcrp1-transfected cells were kindly provided by Dr. Alfred H. Schinkel (The Netherlands Cancer Institute). Cells were cultured in Dulbecco's modified Eagle's medium supplemented with 10% fetal bovine serum (Sigma-Aldrich), penicillin (100 U/ml), streptomycin (100 μg/ml), and amphotericin B (250 ng/ml; Sigma-Aldrich) and maintained at 37°C with 5% CO_2 under humidifying conditions.

Intracellular Accumulation Studies in MDCKII Cells. The accumulation studies were done in 24-well polystyrene plates (Thermo Fisher Scientific, Waltham, MA). The wild-type and MDR1- or Bcrp1-transfected cells were seeded at a density of 2×10^5 cells/well. The medium was changed on alternate days until the cells formed confluent monolayers. On the day of the experiment, the medium was aspirated, and the monolayer was washed twice with 1 ml of prewarmed (37°C) assay buffer. The cells were preincubated with 1 ml of assay buffer for 30 min, after which the buffer was aspirated and the experiment initiated by adding 1 ml of a tracer solution of radiolabeled [^{14}C]gefitinib to each well. The plates were continuously agitated at 60 rpm in an orbital shaker that was maintained at 37°C for the duration of the experiment. At the end of the 1-h accumulation period, the assay buffer containing the radiolabeled drug was aspirated from all wells, and the cells were washed twice with 1 ml of ice-cold phosphate-buffered saline. Cells were then solubilized using 0.5 ml of a 1% Triton X-100 solution. A 150-μl sample of solubilized cell fractions was drawn from each well in duplicate; 4 ml of scintillation fluid (ScintiSafe Econo cocktail; Thermo Fisher Scientific) was added; and the radioactivity associated with the cell fractions was determined by liquid scintillation counting (LS-6500; Beckman Coulter, Inc., Fullerton, CA). The BCA protein assay (Pierce Biotechnology, Inc., Rockford, IL) was used to determine the protein concentration in the cell fractions and was used to normalize the radioactivity in each well. Drug accumulation in cells was expressed as percentage of the accumulated radioactivity measured in the wild-type control cells (disintegration per minute) per microgram of protein. For inhibition studies, the cells were treated with selective inhibitors during both the preincubation and accumulation periods: 1 μM LY335979 for P-gp and 200 nM Ko143 for BCRP (Dantzig et al., 1999; Allen et al., 2002). The stock solutions

for all of the inhibitors used were prepared in dimethyl sulfoxide (DMSO) and diluted using assay buffer to obtain working solutions, so that the final concentration of DMSO was less than 0.1%.

Directional Flux across MDCKII Monolayers. Six-well Transwell plates (Corning Life Sciences, Lowell, MA) were used in the permeability studies. Cells were seeded at a density of 2×10^5 cells/well on the polyester semipermeable membrane supports, and the medium was changed on alternate days until the cells formed confluent monolayers. On the day of experiment, the monolayers were washed with 2 ml of prewarmed (37°C) assay buffer. After a 30-min preincubation period, the experiment was initiated by adding a tracer solution of the radiolabeled drug [^{14}C]gefitinib in assay buffer to the donor side (apical side, 1.5 ml; basolateral side, 2.6 ml). Fresh assay buffer was added to the receiver side, and 200 μl was sampled from the receiver compartment at 0, 10, 20, 30, 45, 60, and 90 min. The volume sampled was immediately replaced with fresh assay buffer. Additional samples were drawn at 0 and 90 min from the donor compartment. The amount of radioactivity in the samples was determined using liquid scintillation counting. The apical compartment represented the donor for determination of apical-to-basolateral (A-to-B) flux, whereas for determination of basolateral-to-apical (B-to-A) flux, the donor was the basolateral compartment and the apical compartment was sampled at the aforementioned times. When an inhibitor was used in the flux study, the cell monolayers were preincubated with the inhibitor (1 μM LY335979 or 200 nM Ko143) for 30 min, followed by determination of A-to-B and B-to-A flux with the inhibitor present in both compartments throughout the course of the experiment. The apparent permeability (P_{app}) was calculated by the following equation,

$$P_{app} = \frac{\left(\frac{dQ}{dt}\right)}{A \times C_0} \quad (1)$$

where dQ/dt is the mass transport rate (determined from the slope of the amount transported versus time plot), A is the apparent surface area of the cell monolayer (4.67 cm^2), and C_0 is the initial donor concentration. The efflux ratio was defined as the ratio of P_{app} in the B-to-A direction to the P_{app} in the A-to-B direction and gives an indication of the magnitude of P-gp or BCRP-mediated efflux. The corrected flux ratio was determined by dividing the efflux ratio in the Bcrp1 or MDR1 transfected cells by the efflux ratio in the corresponding wild-type cells.

In Vivo Studies

Animals. All animals used in this study were from Taconic Farms, Inc. (Germantown, NY). Animals used were male *Mdr1a/b(−/−)* (P-gp knockout), *Bcrp1(−/−)* (Bcrp1 knockout), *Mdr1a/b(−/−) Bcrp1(−/−)* (triple knockout), and wild-type mice of a FVB/N genetic background and were 8 to 10 weeks old at the time of the experiment. Animals were maintained under temperature-controlled conditions with a 12-h light/dark cycle and unlimited access to food and water. All studies were conducted according to the guidelines set by the *Principles of Laboratory Animal Care* (National Institutes of Health) and were approved by The Institutional Animal Care and Use Committee (IACUC) of the University of Minnesota.

Brain Distribution of Gefitinib in FVB Mice. The dose formulation of gefitinib was prepared on the day of experiment at a concentration of 5 mg/ml. Gefitinib was suspended in 1% polysorbate 80 solution in saline or in a vehicle consisting of 10% DMSO, 35% propylene glycol, 5% ethanol, and 50% saline. All mice received a 25 mg/kg oral dose of gefitinib via oral gavage.

In the first study, wild-type and *Mdr1a/b(−/−) Bcrp1(−/−)* mice were administered an oral dose of gefitinib (1% polysorbate 80), after which blood and brain were sampled at 15, 30, 60, 90, 120, and 240 min after dose ($n = 4$ at each time point). At the desired time point, animals were euthanized using a CO_2 chamber. Blood was collected by cardiac puncture and transferred to heparinized tubes. Plasma was isolated from blood by centrifugation at 3000 rpm for 10 min at 4°C. Whole brain was immediately removed from the skull, rinsed with cold saline, and flash-frozen in liquid nitrogen. Plasma and brain specimens were stored at −80°C until analysis by liquid chromatography-MS/MS.

In another study, wild-type mice received an oral dose of gefitinib (10% DMSO, 35% propylene glycol, 5% ethanol, and 50% saline) with or without an intravenous dose of 10 mg/kg elacridar (GF120918) 30 min before administration of gefitinib. Blood and brain were sampled at 15, 30, 60, 90, and 120 min after dose as described above ($n = 4$ at each time point). Gefitinib brain distribution was also studied after oral administration in a group of wild-type, *Mdr1a/b(−/−)*, *Bcrp1(−/−)*, and *Mdr1a/b(−/−) Bcrp1(−/−)* mice and in wild-type mice that received 25 mg/kg LY335979 (20% ethanol, 80% saline), 10 mg/kg Ko143 (20% DMSO, 80% saline), or 10 mg/kg GF120918 (40% propylene glycol, 30% DMSO, 30% saline) intravenously 30 min before an oral gefitinib dose. Blood and brain were sampled at 90 min after dose ($n = 4$ at each time point).

Steady-State Brain Distribution of Gefitinib. Alzet osmotic mini pumps (Durect Corporation, Cupertino, CA) were used to study the steady-state brain and plasma levels of gefitinib. A 70 mg/ml solution of gefitinib in DMSO was filled in the mini pumps (model 1003D), and the pumps were equilibrated by soaking them overnight in sterile saline solution at 37°C. The pump operated at a flow rate of 1 μl/h, yielding an infusion rate of 70 μg/h. Wild-type and *Mdr1a/b(−/−) Bcrp1(−/−)* mice were anesthetized by intraperitoneal administration of 100 mg/kg ketamine and 10 mg/kg xylazine (Boynton Health Service Pharmacy, Minneapolis, MN). The abdominal cavity was shaved and cleaned. Next, a small midline incision was made in the lower abdomen under the rib cage. A small incision was then made in the peritoneal wall directly beneath the cutaneous incision, and the primed pump was inserted into the peritoneal cavity. The musculoperitoneal layer was closed with sterile absorbable sutures, and the skin incision was closed using sterile wound clips. The animals were allowed to recover on a heated pad. Gefitinib half-life in mice has been reported to be approximately 1 h (Wang et al., 2008), so an infusion lasting 24 h was considered to be sufficient to attain steady state in both brain and plasma. The animals were euthanized 24 and 48 h after surgery followed by collection of brain and blood as described earlier.

Determination of Gefitinib Concentrations in Plasma and Brain by liquid chromatography-MS/MS. Before analysis, frozen samples were thawed at ambient temperature. Brain samples were homogenized with 3 volumes of 5% bovine serum albumin in phosphate-buffered saline with use of a tissue homogenizer (Thermo Fisher Scientific). A 50-μl aliquot of plasma and a 100-μl aliquot of brain homogenate were used for analysis. Plasma and brain samples were spiked with 10 ng of dasatinib as internal standard followed by liquid-liquid extraction using a 200-μl buffer (pH 11, sodium hydroxide/sodium bicarbonate, 50:50) and 1 ml of ice-cold ethyl acetate. Samples were shaken vigorously on a mechanical shaker for 10 min and centrifuged at 5000 rpm for 15 min at 4°C to separate the organic layer. A volume of 750 μl of the top organic layer was transferred to fresh polypropylene tubes and dried under nitrogen. Samples were reconstituted in 100-μl mobile phase and transferred to glass auto sampler vials. A volume of a 5-μl sample was injected in the high-performance liquid chromatography system using a temperature controlled autosampling device maintained at 10°C. Chromatographic analysis was performed using an Agilent model 1200 separation system (Agilent Technologies, Santa Clara, CA). Separation of analytes was achieved using an Agilent Eclipse XDB-C18 RRHT threaded column (4.6 mm inner diameter × 50 mm) packed with a 1.8-μm ZORBAX Rx-SIL silica stationary phase. The mobile phase used for the chromatographic separation was composed of acetonitrile:20 mM ammonium formate (containing 0.1% formic acid, pH adjusted to 4 with ammonium hydroxide) (32:68 v/v) and was delivered at a flow rate of 0.25 ml/min. The column effluent was monitored using a TSQ Quantum 1.5 detector (Thermo Fisher Sci-

entific). The instrument was equipped with an electrospray interface and controlled by the Xcalibur version 2.0.7 data system. The samples were analyzed using an electrospray probe in the positive ionization mode operating at a spray voltage of 4500 V for both gefitinib and dasatinib (internal standard). Samples were introduced into the interface through a heated nebulized probe at 300°C. The spectrometer was programmed to allow the $[MH]^+$ ion of gefitinib at *m/z* 446.9 and that of internal standard at *m/z* 488 to pass through the first quadrupole (Q1) and into the collision cell (Q2). The collision energy was set at 9 V for gefitinib and 16 V for dasatinib. The product ions for gefitinib (*m/z* 128.1) and the internal standard (*m/z* 401) were monitored through the third quadrupole (Q3). The scan width and scan time for monitoring the two product ions were 1.5 *m/z* and 0.5 s, respectively. The sensitivity of our assay was at least 7.5 ng/ml with a corresponding coefficient of variation of approximately 10%.

Evaluating Blood-Brain Barrier Integrity in FVB Wild-type and *Mdr1a/b(−/−) Bcrp1(−/−)* Mice. A group of FVB wild-type and *Mdr1a/b(−/−) Bcrp1(−/−)* mice received an intravenous dose of 5 μCi of [^{14}C]sucrose ($n = 4$). Another group received an intravenous dose of 2.5 μCi of [^{14}C]inulin ($n = 4$). Blood and whole brain were harvested at 10 min after dose. Brains were homogenized as described earlier. Scintillation fluid (4 ml of ScintiSafe Econo 1 cocktail; Thermo Fisher Scientific) was added to 100 μl of brain or 20 μl of plasma specimens and counted with a liquid scintillation counter (LS-6500; Beckman Coulter Inc.) to determine the radioactivity associated with sucrose and inulin in the samples. Sucrose and inulin concentrations in brain and plasma were determined. Brain space was calculated as the ratio of the brain concentration (nanocurie per gram) to the plasma concentration (nanocurie per milliliter) and expressed as the percentage of brain volume (microliters) exposed to the two compounds.

Statistical Analysis

Statistical analysis was conducted using SigmaStat, version 3.1 (Systat Software, Inc., Point Richmond, CA). Statistical comparisons between two groups were made by using two-sample *t* test at $p < 0.05$ significance level. Multiple groups were compared by one-way analysis of variance with the Holm-Sidak post-hoc test for multiple comparisons at a significance level of $p < 0.05$.

Results

Intracellular Accumulation of Gefitinib. Accumulation of gefitinib in MDCKII WT and P-gp or Bcrp1-transfected cells was studied. A positive control, [^{3}H]vinblastine for P-gp or [^{3}H]prazosin for BCRP, was used in all accumulation experiments. As seen in Fig. 1A, [^{3}H]prazosin accumulation in the Bcrp1-transfected cells was significantly lower compared with the wild-type cells ($p < 0.001$). Likewise, accumulation of [^{3}H]vinblastine was significantly lower in the MDR1-transfected cells ($p < 0.001$) compared with WT (Fig. 1B). Accumulation of gefitinib in the Bcrp1-transfected cells was significantly lower than that in the wild-type cells (approximately 3% of WT control, $p < 0.001$). This difference in accumulation between the two cell types was abolished upon treatment with the BCRP-specific inhibitor Ko143 (200 nM) (Fig. 1A). In the MDR1-transfected cells, accumulation of gefitinib was 50% lower than that in the wild-type cells ($p < 0.001$). Treatment with the P-gp inhibitor LY335979 (1 μM) decreased the difference in accumulation (Fig. 1B).

Directional Permeabilities of Gefitinib across MDCKII Monolayers. MDCKII wild-type and Bcrp1 or MDR1-transfected cells were used to determine the directional flux of [^{14}C]gefitinib. Figure 2A demonstrates the directionality in permeability of gefitinib across wild-type and

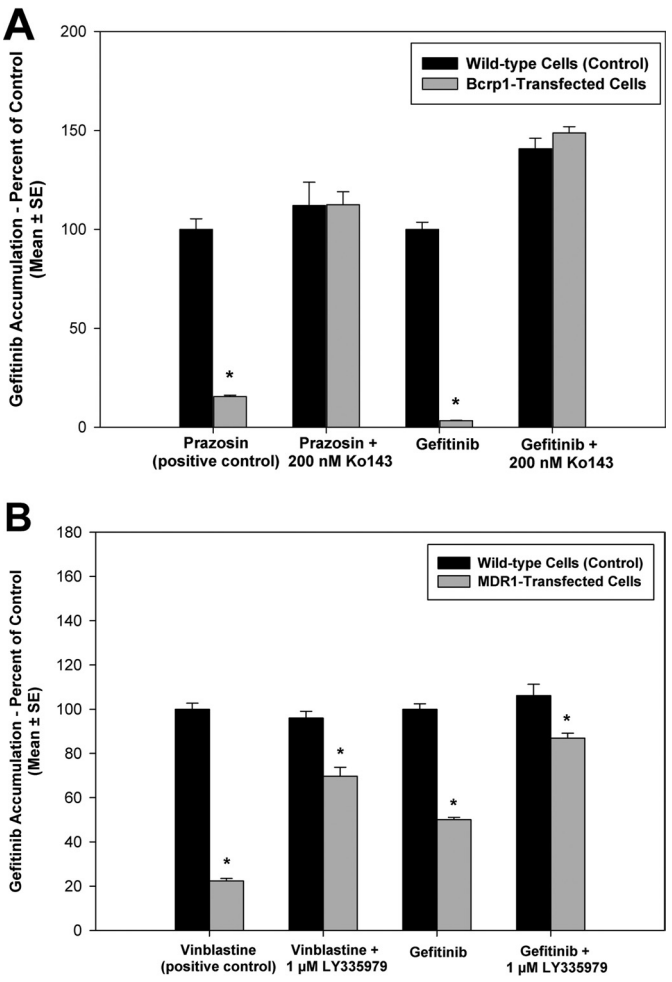

Fig. 1. Intracellular accumulation of [^{14}C]gefitinib in MDCKII cells. A, accumulation in wild-type (black bar) and Bcrp1-transfected (gray bar) cells. Gefitinib accumulation in the Bcrp1-transfects was approximately 30-fold lower compared with that in wild-type cells (*, $p < 0.001$). This difference in accumulation was abolished when BCRP was inhibited using the specific inhibitor Ko143. B, accumulation in wild-type (black bar) and MDR1-transfected (gray bar) cells. Gefitinib accumulation was significantly lower in the MDR1-transfected cells compared with wild type (*, $p < 0.001$). Treatment with LY335979 reduced the difference in accumulation between the two cell types. Results presented as mean ± S.E., $n = 18$.

Bcrp1 monolayers. The B-to-A permeability of gefitinib in the Bcrp1 cells was significantly greater than the permeability in the A-to-B direction ($p < 0.001$) yielding an efflux ratio of 55. This directionality in transport was abolished when the cells were treated with Ko143 (200 nM), such that there was no significant difference between the A-to-B and B-to-A permeabilities (efflux ratio = approximately 1). In the wild-type cells, there was no difference in the permeability of gefitinib in either direction, with an efflux ratio of approximately 1 in the control (no Ko143 treatment) and the Ko143-treated cells. The corrected efflux ratio was approximately 34 in the control and 1.2 in the cells treated with the BCRP inhibitor Ko143. In the MDR1-transfected cells, the permeability was significantly enhanced in the B-to-A direction compared with the A-to-B permeability ($p < 0.001$), with an efflux ratio of 8.4 (Fig. 2B). The P-gp inhibitor LY335979 reversed the directionality in flux due to P-gp, such that there was no significant difference in the permeability of gefitinib in both directions, and the efflux ratio decreased to 1. Again, the B-to-A

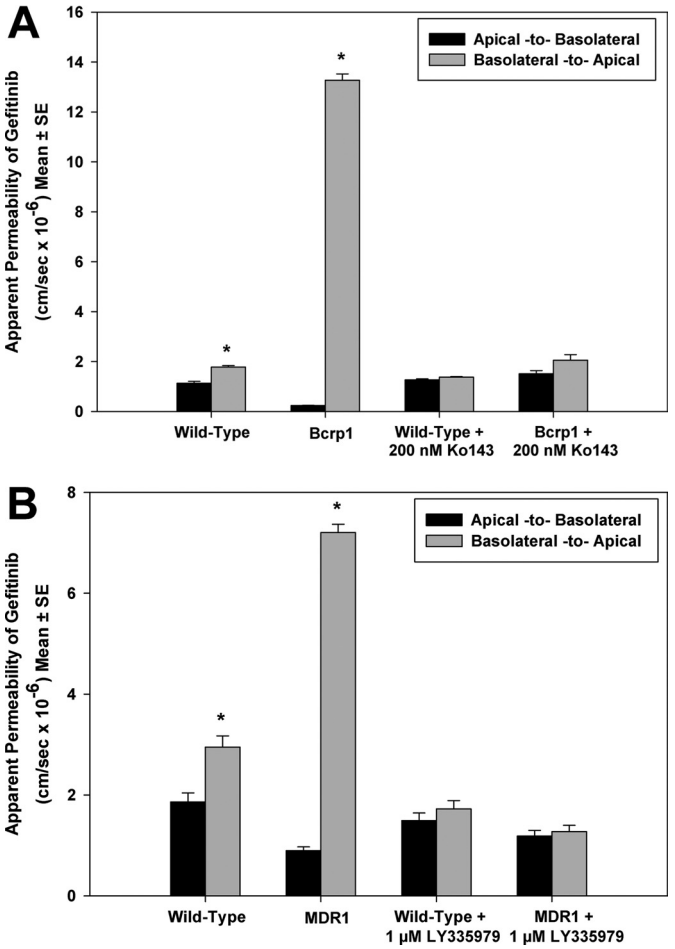

Fig. 2. Flux of [^{14}C]gefitinib across MDCKII cell monolayers. A, gefitinib permeability across wild-type and Bcrp1-transfected cells. In the Bcrp1-transfected cells, the B-to-A permeability (gray bar) of gefitinib was significantly greater than the A-to-B permeability (black bar) (*, $p < 0.001$). This directionality in transport was abolished when cells were treated with the BCRP-specific inhibitor Ko143. B, permeability across wild-type and MDR1-transfected cells. The B-to-A permeability (gray bar) was significantly greater than the A-to-B permeability (black bar) in the MDR1- transfected cells (*, $p < 0.001$). P-gp inhibition by LY335979 abolished this directionality in transport, such that there was no difference in permeability between the two directions. Results presented as mean ± S.E., $n = 9$.

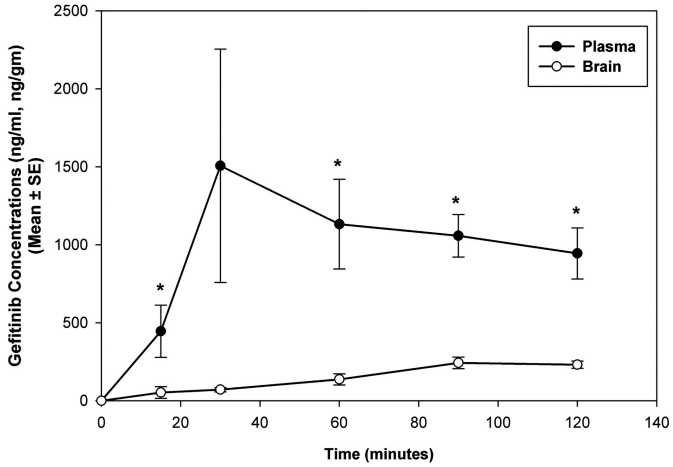

Fig. 3. Brain and plasma concentrations of gefitinib in FVB wild-type mice after a 25 mg/kg oral dose of gefitinib. Brain gefitinib concentrations (○) were significantly lower than the plasma concentrations (●), demonstrating the limited brain penetration of gefitinib (mean ± S.E., $n = 4$, *, $p < 0.05$ compared with wild-type control).

and A-to-B permeability was similar in the corresponding wild-type cells. The corrected efflux ratio was approximately 5.1 in the control and 0.9 in the cells treated with LY335979.

Brain Distribution of Gefitinib in Wild-Type and *Mdr1a/b(−/−) Bcrp1(−/−)* Mice. We investigated the effect of P-glycoprotein and BCRP on the brain distribution of gefitinib by use of wild-type and transgenic mouse models. Brain distribution after an oral dose of 25 mg/kg gefitinib was determined in FVB wild-type and *Mdr1a/b(−/−) Bcrp1(−/−)* mice. Brain concentrations of gefitinib were significantly lower than the plasma concentrations in the wild-type mice ($p < 0.05$), resulting in a brain-to-plasma (B/P) concentration ratio of less than 0.15 at all of the measured time points (Fig. 3). However, gefitinib brain concentrations were significantly enhanced in the *Mdr1a/b(−/−) Bcrp1(−/−)* mice compared with those in the wild-type mice ($p < 0.05$; Fig. 4A). The brain-to-plasma concentration ratio was significantly greater in the *Mdr1a/b(−/−) Bcrp1(−/−)* mice at all of the measured time points ($p < 0.001$). The B/P ratio was on average 16-fold higher in the *Mdr1a/b(−/−) Bcrp1(−/−)* mice compared with the wild-type mice (Fig. 4B). Plasma concentrations of gefitinib in the *Mdr1a/b(−/−) Bcrp1(−/−)* mice were not significantly different compared with the plasma concentrations in the wild-type mice.

Dual P-gp and BCRP Inhibitor Elacridar Enhances Brain Distribution of Gefitinib. We investigated whether pharmacological inhibition of P-gp and BCRP at the blood-brain barrier enhances the brain exposure of gefitinib in FVB wild-type mice. The dual P-gp and BCRP inhibitor elacridar (GF120918) was used for this purpose. Brain gefitinib concentrations were greater in the elacridar-treated group compared with control (Fig. 5A). The B/P was significantly greater in the elacridar-treated wild-type mice compared with the control ($p < 0.05$; Fig. 5B). The brain-to-plasma ratio increased by more than 4-fold when elacridar was administered along with gefitinib, reaching values greater than 1 at the later time points. This indicates that brain distribution of gefitinib can be significantly improved by concurrent administration of a dual inhibitor such as elacridar.

Effect of Pharmacological Inhibition and Genetic Deletion of P-gp and BCRP. We studied the brain distribution of gefitinib in wild-type, *Mdr1a/b(−/−)*, *Bcrp1(−/−)*, and *Mdr1a/b(−/−) Bcrp1(−/−)* mice and in wild-type mice that were pretreated with pharmacological inhibitors of P-gp (LY335979), BCRP (Ko143), and the dual P-gp/BCRP inhibitor elacridar. Figure 6 shows the brain-to-plasma ratios of gefitinib when P-gp and BCRP were pharmacologically inhibited or genetically deleted. Use of LY335979 and Ko143 did not result in any significant change in the B/P ratio of gefitinib; however, the B/P ratio increased by approximately 6-fold in the wild-type mice that were pretreated with the dual inhibitor elacridar ($p < 0.05$). Likewise, in the gene knockout group, the B/P ratio increased by approximately 4-fold in the *Mdr1a/b(−/−)* mice ($p < 0.05$). Although there was no change in the B/P ratio in the *Bcrp1(−/−)* mice, the ratio increased by greater than 18-fold in the *Mdr1a/b(−/−)Bcrp1(−/−)* mice ($p < 0.001$).

Steady-State Brain Distribution of Gefitinib. Table 1 summarizes the results from steady-state brain and plasma distribution of gefitinib after a continuous intraperitoneal infusion. In the wild-type mice, steady-state brain concentra-

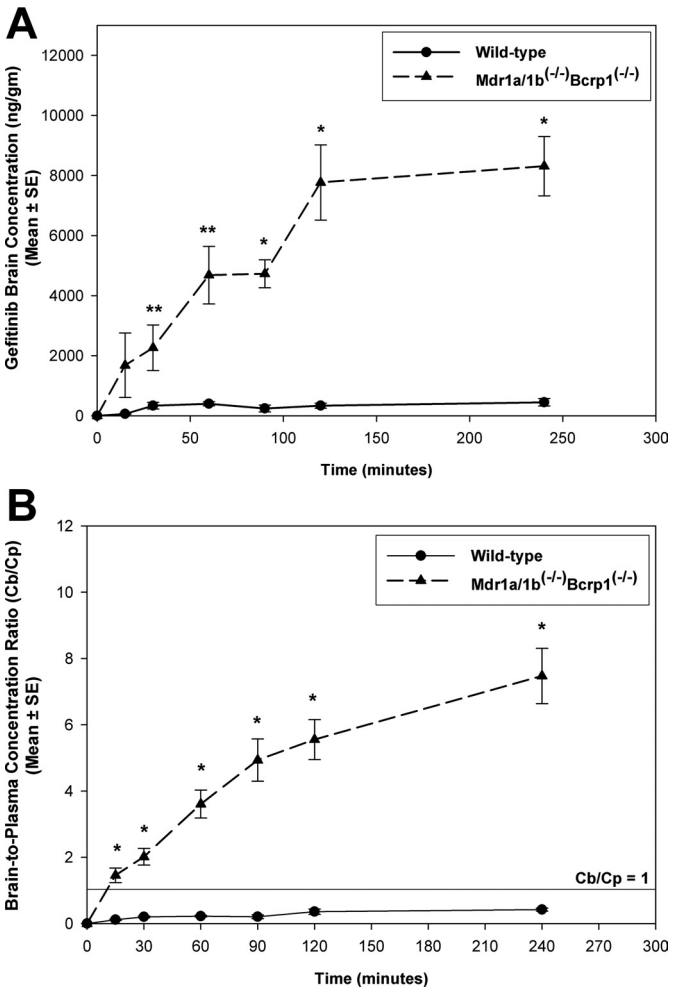

Fig. 4. Brain distribution of gefitinib in wild-type and *Mdr1a/b(−/−) Bcrp1(−/−)* FVB mice after an oral dose of 25 mg/kg gefitinib. A and B, brain concentrations (A) and corresponding B/P concentration ratios (B) of gefitinib in wild-type (●) and *Mdr1a/b(−/−) Bcrp1(−/−)* (▲) mice. Brain concentrations in the *Mdr1a/b(−/−)Bcrp1(−/−)* mice were significantly greater than the wild type. The B/P ratios increased by greater than 16-fold in the *Mdr1a/b(−/−) Bcrp1(−/−)* mice, indicating the enhancement in brain distribution of gefitinib due to absence of P-gp and BCRP at the BBB. Results are represented as mean ± S.E. (**, $p < 0.05$, *, $p < 0.001$ compared with wild-type control).

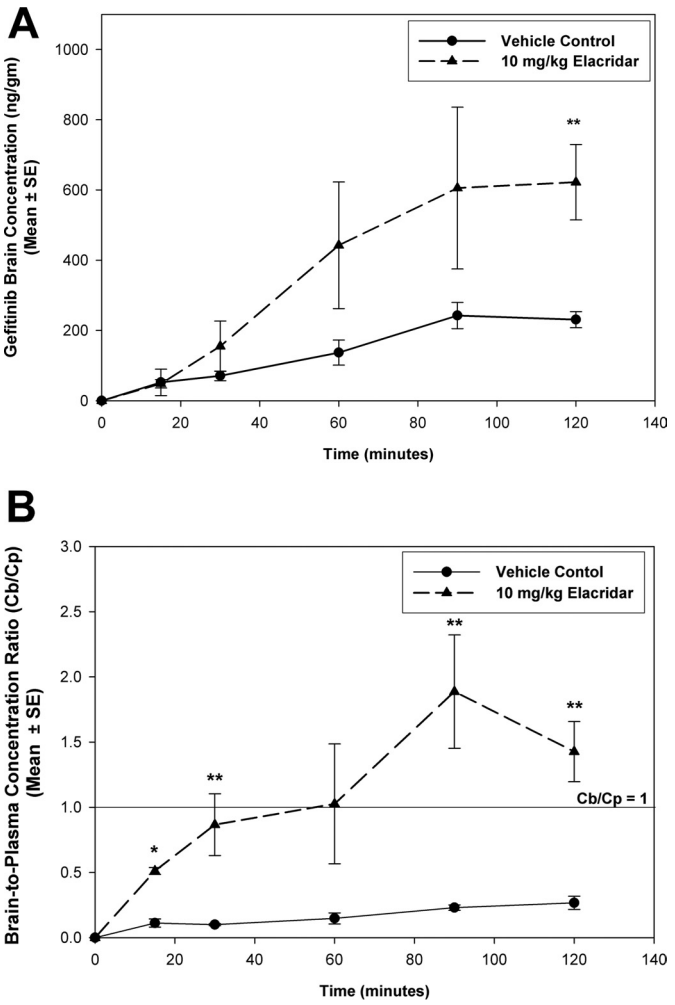

Fig. 5. Effect of P-gp and BCRP inhibition on brain distribution of gefitinib. A and B, brain concentrations (A) and corresponding B/P concentration ratios (B) of gefitinib in the vehicle-treated (●) and elacridar-treated (▲) wild-type mice. Brain concentrations increased in the wild-type mice when elacridar was administered before gefitinib. The B/P ratios were also significantly greater in the elacridar-treated group, suggesting that dual inhibitors such as elacridar can be used to improve brain penetration of substrate drugs. Results are represented as mean ± S.E. (**, $p < 0.05$, *, $p < 0.001$ compared with vehicle control).

tions of gefitinib were 15-fold lower than the corresponding plasma concentrations ($p < 0.001$). The brain-to-plasma ratio was approximately 0.1 at both the measured time points, indicating a brain tissue partition coefficient of 10% in the wild-type mice. In the *Mdr1a/b(−/−) Bcrp1(−/−)* mice, brain concentrations were approximately 7-fold greater compared with the plasma concentrations ($p < 0.001$). Steady-state brain concentrations in the *Mdr1a/b(−/−) Bcrp1(−/−)* mice increased more than 50-fold compared with that in the wild-type mice ($p < 0.001$). The corresponding brain-to-plasma ratios in the *Mdr1a/b(−/−) Bcrp1(−/−)* mice were approximately 7, indicating a 70-fold increase in brain partitioning of gefitinib compared with the wild type. There was no difference in the brain-to-plasma ratios between the 24- and 48-h time points in the two mice groups.

Blood-Brain Barrier Integrity in FVB *Mdr1a/b(−/−) Bcrp1(−/−)* Mice. The integrity of the BBB in the *Mdr1a/b(−/−) Bcrp1(−/−)* mice was evaluated to ensure that the dramatic increase in brain distribution of gefitinib observed in the triple knockout mice was not a result of a leaky blood-brain barrier (compromised tight junctions). This was done by determining the brain spaces of [^{14}C]sucrose and [^{14}C]inulin. At short time points after dose, both inulin and sucrose are limited to the vasculature under normal physiological conditions and therefore are used as markers of intravascular space. The brain spaces of [^{14}C]sucrose and [^{14}C]inulin in the *Mdr1a/b(−/−) Bcrp1(−/−)* mice were not statistically different from those in the wild-type mice. The brain sucrose space at 10 min was 2.2 ± 0.2% in the wild-type mice compared with 1.9 ± 0.3% in the *Mdr1a/b(−/−) Bcrp1(−/−)* mice. Likewise, the brain space of [^{14}C]inulin was 2.0 ± 0.3% in the wild-type mice and 2.1 ± 0.6% in the *Mdr1a/b(−/−) Bcrp1(−/−)* mice (Fig. 7). The finding confirmed that there was no change in the integrity of the tight junctions that form the BBB in the *Mdr1a/b(−/−)Bcrp1(−/−)* mice. This suggests that the cumulative change in brain distribution of gefitinib in these mice is due to the simultaneous absence of both drug efflux systems.

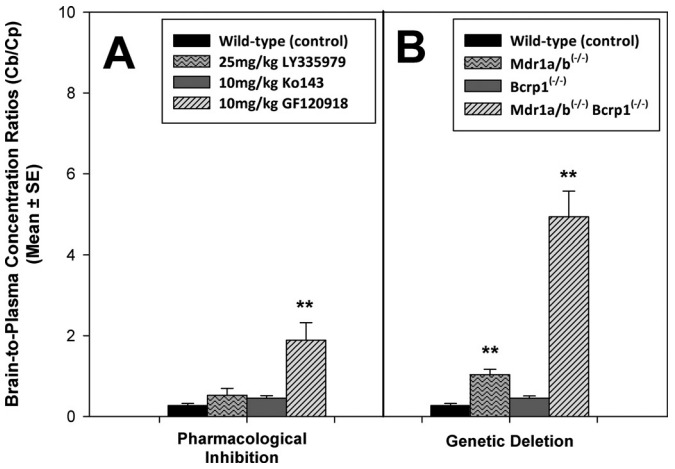

Fig. 6. A, effect of pharmacological inhibition of drug efflux transporters on brain distribution of gefitinib in wild-type FVB mice. Wild-type mice received 25 mg/kg gefitinib via oral gavage 30 min after intravenous administration of 25 mg/kg LY335979, 10 mg/kg Ko143, or 10 mg/kg GF120918 (elacridar). B, effect of genetic deletion of drug efflux transporters on brain distribution of gefitinib in FVB mice. Wild-type, *Mdr1a/b(−/−)*, *Bcrp1(−/−)*, and *Mdr1a/b(−/−) Bcrp1(−/−)* mice were administered 25 mg/kg gefitinib. Whole-brain tissue was collected at 90 min after dose ($n = 4$ at each time point) and analyzed for gefitinib. The values are presented as mean ± S.E. (**, $p < 0.05$, compared with wild-type control).

Discussion

The EGFR pathway has been an attractive target because it is dysregulated in a significant fraction of malignant gliomas through overexpression, amplification, and activating mutations (Rich et al., 2004). Moreover, recent studies have demonstrated that EGFRvIII is required for tumor maintenance in glioma (Mukasa et al., 2010). The EGFR tyrosine kinase inhibitor gefitinib has been evaluated in a number of clinical trials for GBM; however, results have been disappointing (Rich et al., 2004; Lieberman et al., 2004). The failure of gefitinib raises questions pertaining to delivery of drug to its target. Active efflux at the BBB could prevent drugs from attaining therapeutic levels in the brain and is probably one of the main reasons behind resistance to chemotherapy. It has been shown that several other tyrosine kinase inhibitors are avid substrates for P-gp and BCRP and that their brain distribution is limited due to active efflux out of the brain (Dai et al., 2003; Chen et al., 2009; Lagas et al., 2009; Polli et al., 2009). Whether gefitinib crosses the BBB to achieve therapeutic levels in the CNS is an important question that has remained unanswered. We have raised this question herein and demonstrated that gefitinib is a substrate of the ABC transporters P-gp and BCRP and that these two efflux proteins actively efflux gefitinib at the BBB, thereby limiting its brain penetration. We have further demonstrated that steady-state brain partitioning improved by greater than 70-fold due to absence of both P-gp and BCRP in the *Mdr1a/b(−/−) Bcrp1(−/−)* mice and that inhibition of these two transporters by use of a dual inhibitor such as elacridar can be a useful therapeutic strategy to improve brain distribution of gefitinib.

In vitro studies conducted in immortalized MDCKII cells that stably overexpress human P-gp or murine BCRP demonstrated that gefitinib is a substrate of the two efflux pumps. It has been reported that gefitinib is an inhibitor of P-gp and BCRP and that concurrent administration increases the bioavailability of topotecan (Leggas et al., 2006). Our study conclusively shows that gefitinib is a substrate for these two transporters. One explanation for the inhibitory effect seen could be given by the high gefitinib concentrations used by Leggas et al. (2006) in the above-mentioned study. It is also possible that gefitinib competes with other substrates to bind with P-gp and BCRP and saturates the transporters, thus leading to their inhibition.

In vivo studies using FVB wild-type mice showed that CNS distribution of gefitinib across the blood-brain barrier is significantly limited. Brain concentrations were on average 18-fold higher in the *Mdr1a/b(−/−) Bcrp1(−/−)* mice than in the wild-type mice. Steady-state brain-to-plasma ratios increased from approximately 0.1 in the wild-type mice to approximately 7 in the *Mdr1a/b(−/−) Bcrp1(−/−)* mice. This dramatic 70-fold increase in the partitioning of the brain indicates the significant impact the two transporters have on the brain distribution of gefitinib.

The dramatic increase in brain gefitinib concentrations in the *Mdr1a/b(−/−) Bcrp1(−/−)* mice suggested that inhibition of P-gp and BCRP might be an effective way to improve brain distribution of gefitinib. Therefore, we studied the influence of the dual P-gp and BCRP inhibitor elacridar on the brain distribution of gefitinib in FVB wild-type mice. Treatment with elacridar resulted in enhanced brain levels of gefitinib in the wild-type mice. This finding demonstrates the improvement in delivery of gefitinib to the brain resulting from pharmacological inhibition of active efflux at the BBB. It is noteworthy that plasma concentrations of gefitinib were not increased in the *Mdr1a/b(−/−) Bcrp1(−/−)* mice or in the elacridar-treated wild-type mice compared with control wild-type mice, suggesting that, under these experimental conditions, P-gp and BCRP do not limit oral uptake of gefitinib. This finding is in agreement with other studies that report that oral absorption of tyrosine kinase inhibitors, such

TABLE 1

Steady-state brain distribution of gefitinib in wild-type and *Mdr1a/b(−/−) Bcrp1(−/−)* FVB mice after a continuous intraperitoneal infusion of gefitinib

Steady-state brain concentrations were 16-fold lower than the plasma concentrations in the wild-type mice. Brain concentrations at steady-state in the *Mdr1a/b(−/−) Bcrp1(−/−)* mice were 7-fold greater than the plasma concentrations and up to 100-fold greater than the brain concentrations in wild-type mice (mean ± S.E.).

Group	Time	n	Plasma C_{ss}	Brain C_{ss}	Brain-to-Plasma Ratio
	h		$\mu g/ml$	$\mu g/g$	
Wild-type (control)	24	5	0.49 ± 0.08	0.03 ± 0.01*	0.07 ± 0.02
	48	4	0.21 ± 0.05	0.01 ± 0.01*	0.10 ± 0.05[a]
Mdr1a/b(−/−)Bcrp1(−/−)	24	4	0.24 ± 0.07	1.7 ± 0.5*†	7.3 ± 0.5†
	48	4	0.19 ± 0.10	1.2 ± 0.6*†	7.1 ± 0.9†[a]

*, $p < 0.05$ compared to plasma; †, $p < 0.05$ compared to wild type.
[a] ns, not significant compared to 24-h time point.

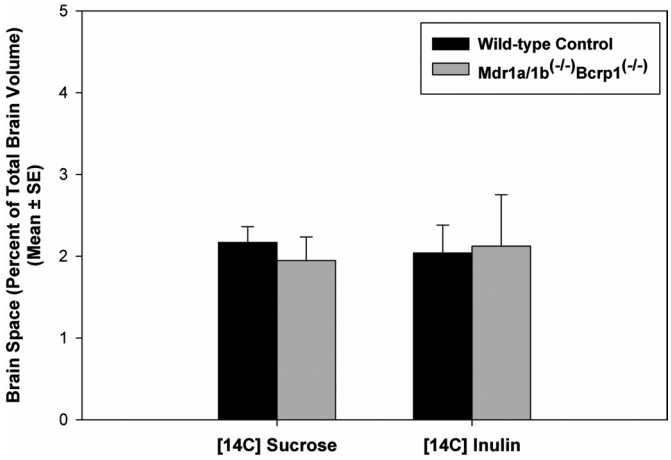

Fig. 7. Integrity of the blood-brain barrier in *Mdr1a/b(−/−) Bcrp1(−/−)* mice. Brain spaces of sucrose and inulin in wild-type (black bar) and *Mdr1a/b(−/−) Bcrp1(−/−)* (gray bar) mice. The brain spaces of sucrose or inulin in the *Mdr1a/b(−/−) Bcrp1(−/−)* mice were similar to those in the wild-type mice, indicating that the BBB is intact in these mice. The values are presented as mean ± S.E. (n = 4).

as dasatinib and erlotinib, is not influenced by P-gp and BCRP (Kamath et al., 2008; Lagas et al., 2010).

In the study to determine the relative contribution of P-gp and BCRP in active efflux of gefitinib, pharmacological inhibition of BCRP by Ko143 or genetic deletion in *Bcrp1(−/−)* mice did not result in any significant increase in brain levels of gefitinib. Brain concentrations and the brain-to-plasma ratios increased by greater than 3-fold when P-gp was absent in the *Mdr1a/b(−/−)* mice. More importantly, concomitant inhibition of P-gp and BCRP by elacridar resulted in an approximately 6-fold increase in the brain-to-plasma ratio, whereas the absence of both transporters in the *Mdr1a/b(−/−) Bcrp1(−/−)* mice had an even greater effect with the B/P ratio increasing by greater than 18-fold. This indicates that P-gp seems to be the dominant transporter when it comes to efflux of gefitinib from the brain. However, the fact that brain concentrations increase only marginally when P-gp is inhibited or absent suggests that BCRP efflux may compensate for the loss of P-gp. This is highlighted in the *Mdr1a/b(−/−) Bcrp1(−/−)* mice or by the use of elacridar, which resulted in a greater than additive increase in brain gefitinib levels. This is consistent with previous reports for dasatinib (Chen et al., 2009; Lagas et al., 2009) and other published reports for tyrosine kinase inhibitors, including imatinib and lapatinib (Oostendorp et al., 2009; Polli et al., 2009). The in vivo finding that BCRP by itself does not influence brain penetration of gefitinib is in agreement with reports for other tyrosine kinase inhibitors. One explanation for this could be the presence of significantly low levels of BCRP in the rodent and human BBB compared with overexpressing cell lines as reported by Lee et al. (2007). Difference in protein levels can account for the discrepancies between the in vitro cell and the in vivo models (Lee et al., 2007). It is also possible that there are differences in the capacities of the two transporters at the BBB where P-gp might seem to play a predominant role at the BBB.

Previous studies have reported similar findings where the brain concentrations of dual P-gp/BCRP substrates increased dramatically in the *Mdr1a/b(−/−) Bcrp1(−/−)* mice (Polli et al., 2009). This raised questions regarding the validity of the triple knockout mice as a model system to study drug transport to the CNS. Some of these questions pertain to the integrity of the BBB in these mice. We decided to evaluate this by studying the brain distribution of sucrose and inulin. Sucrose and inulin do not readily cross membranes and, under normal conditions shortly after systemic dosing, do not enter the brain to any significant extent. A leakier BBB in the *Mdr1a/b(−/−) Bcrp1(−/−)* mice would result in higher brain levels of these two compounds compared with the wild-type mice. We observed no differences in the brain concentrations of [^{14}C]sucrose and [^{14}C]inulin between the wild-type and *Mdr1a/b(−/−) Bcrp1(−/−)* mice. The brain space was approximately 2% for sucrose and inulin in both wild-type and the *Mdr1a/b(−/−) Bcrp1(−/−)* mice. This confirmed that these mice have an intact blood-brain barrier; therefore, the dramatically high brain concentrations of substrate drugs in these mice are most probably due to the simultaneous absence of P-gp and BCRP at the BBB that would not allow for compensatory transport when one or the other is present.

Limited CNS distribution of gefitinib due to active efflux transport at the BBB can be of significance while trying to elucidate the reasons behind the lack of gefitinib efficacy seen in brain tumors such as GBM. It has been suggested that delivery of gefitinib across the BBB might not be an issue in GBM given that tumor concentrations 10- to 12-fold higher than plasma concentrations have been reported previously (McKillop et al., 2005; Hofer and Frei, 2007). One explanation for this increased tumor penetration of gefitinib can be given by the breakdown of the BBB at the contrast-enhancing tumor core. In addition, although the BBB may be disrupted at or near the core, there is increasing evidence to show that it is still intact near the growing edge of the infiltrative tumor (Fine et al., 2006; Blakeley et al., 2009), the site where invasive tumor-initiating cells reside. Tumor recurrence after surgical removal and radiochemotherapy questions the delivery of drug to the non–tumor-containing areas of brain that may only have limited access to the drug. Brain tumor-initiating cells residing behind an intact BBB can pose significant delivery problems and might be one of the main reasons behind the recurrence of tumor after surgery. Despite recent advances in therapy, malignant glioma remains essentially fatal, with a median survival of 10 to 12 months. There are no studies that examine the failure of gefitinib chemotherapy in GBM that address the lack of drug delivery to the intended molecular target in tumor-initiating cells that reside behind an intact BBB. This lack of adequate delivery may be an important reason for the ineffectiveness of gefitinib in brain tumors such as GBM.

In conclusion, here we have shown that the ATP transporters P-gp and BCRP actively efflux gefitinib at the blood-brain barrier and limit its CNS distribution. We have highlighted that gefitinib is another example where P-gp and BCRP can work together to dramatically limit brain distribution of dual substrates. We have also shown that the tight junctions that form the BBB are intact in the *Mdr1a/b(−/−) Bcrp1(−/−)* mice and that the enhanced CNS distribution seen in these mice is due to the absence of P-gp and BCRP. Finally, coadministration of the dual P-gp/BCRP inhibitor elacridar was able to significantly enhance brain distribution of gefitinib. This can be of importance in therapy for GBM, where limited distribution

to the target tumor cells, i.e., the invasive glioma cells behind an intact blood-brain barrier, might be one of the reasons behind the lack of efficacy seen with gefitinib.

Acknowledgments

We thank AstraZeneca Pharmaceuticals (Macclesfield, Cheshire, UK) for kindly supplying radiolabeled gefitinib.

References

Allen JD, van Loevezijn A, Lakhai JM, van der Valk M, van Tellingen O, Reid G, Schellens JH, Koomen GJ, and Schinkel AH (2002) Potent and specific inhibition of the breast cancer resistance protein multidrug transporter in vitro and in mouse intestine by a novel analogue of fumitremorgin C. *Mol Cancer Ther* **1:**417–425.

Arteaga CL and Johnson DH (2001) Tyrosine kinase inhibitors-ZD1839 (Iressa). *Curr Opin Oncol* **13:**491–498.

Blakeley JO, Olson J, Grossman SA, He X, Weingart J, Supko JG, and New Approaches to Brain Tumor Therapy (NABTT) Consortium (2009) Effect of blood brain barrier permeability in recurrent high grade gliomas on the intratumoral pharmacokinetics of methotrexate: a microdialysis study. *J Neurooncol* **91:**51–58.

Brandes AA, Franceschi E, Tosoni A, Hegi ME, and Stupp R (2008) Epidermal growth factor receptor inhibitors in neuro-oncology: hopes and disappointments. *Clin Cancer Res* **14:**957–960.

CBTRUS (2008) *CBTRUS 2008 Statistical Report: Primary Brain Tumors in the United States*, 2000–2004, Central Brain Tumor Registry of the United States, Hinsdale, IL.

Chen Y, Agarwal S, Shaik NM, Chen C, Yang Z, and Elmquist WF (2009) P-glycoprotein and breast cancer resistance protein influence brain distribution of dasatinib. *J Pharmacol Exp Ther* **330:**956–963.

Ciardiello F and Tortora G (2001) A novel approach in the treatment of cancer: targeting the epidermal growth factor receptor. *Clin Cancer Res* **7:**2958–2970.

Culy CR and Faulds D (2002) Gefitinib. *Drugs* **62:**2237–2248; discussion 2249–2250.

Dai H, Marbach P, Lemaire M, Hayes M, and Elmquist WF (2003) Distribution of STI-571 to the brain is limited by P-glycoprotein-mediated efflux. *J Pharmacol Exp Ther* **304:**1085–1092.

Dantzig AH, Shepard RL, Law KL, Tabas L, Pratt S, Gillespie JS, Binkley SN, Kuhfeld MT, Starling JJ, and Wrighton SA (1999) Selectivity of the multidrug resistance modulator, LY335979, for P-glycoprotein and effect on cytochrome P-450 activities. *J Pharmacol Exp Ther* **290:**854–862.

Davis FG, Kupelian V, Freels S, McCarthy B, and Surawicz T (2001) Prevalence estimates for primary brain tumors in the United States by behavior and major histology groups. *Neuro Oncol* **3:**152–158.

Elkind NB, Szentpétery Z, Apáti A, Ozvegy-Laczka C, Várady G, Ujhelly O, Szabó K, Homolya L, Váradi A, Buday L, et al. (2005) Multidrug transporter ABCG2 prevents tumor cell death induced by the epidermal growth factor receptor inhibitor Iressa (ZD1839, Gefitinib). *Cancer Res* **65:**1770–1777.

Fine RL, Chen J, Balmaceda C, Bruce JN, Huang M, Desai M, Sisti MB, McKhann GM, Goodman RR, Bertino JS Jr, et al. (2006) Randomized study of paclitaxel and tamoxifen deposition into human brain tumors: implications for the treatment of metastatic brain tumors. *Clin Cancer Res* **12:**5770–5776.

Fletcher JI, Haber M, Henderson MJ, and Norris MD (2010) ABC transporters in cancer: more than just drug efflux pumps. *Nat Rev Cancer* **10:**147–156.

Franceschi E, Cavallo G, Lonardi S, Magrini E, Tosoni A, Grosso D, Scopece L, Blatt V, Urbini B, Pession A, et al. (2007) Gefitinib in patients with progressive high-grade gliomas: a multicentre phase II study by Gruppo Italiano Cooperativo di Neuro-Oncologia (GICNO). *Br J Cancer* **96:**1047–1051.

Giaccone G, Herbst RS, Manegold C, Scagliotti G, Rosell R, Miller V, Natale RB, Schiller JH, Von Pawel J, Pluzanska A, et al. (2004) Gefitinib in combination with gemcitabine and cisplatin in advanced non–small-cell lung cancer: a phase III trial–INTACT 1. *J Clin Oncol* **22:**777–784.

Gottesman MM, Fojo T, and Bates SE (2002) Multidrug resistance in cancer: role of ATP-dependent transporters. *Nat Rev Cancer* **2:**48–58.

Herbst RS, Giaccone G, Schiller JH, Natale RB, Miller V, Manegold C, Scagliotti G, Rosell R, Oliff I, Reeves JA, et al. (2004) Gefitinib in combination with paclitaxel and carboplatin in advanced non–small-cell lung cancer: a phase III trial–INTACT 2. *J Clin Oncol* **22:**785–794.

Hofer S and Frei K (2007) Gefitinib concentrations in human glioblastoma tissue. *J Neurooncol* **82:**175–176.

Kamath AV, Wang J, Lee FY, and Marathe PH (2008) Preclinical pharmacokinetics and in vitro metabolism of dasatinib (BMS-354825): a potent oral multi-targeted kinase inhibitor against SRC and BCR-ABL. *Cancer Chemother Pharmacol* **61:**365–376.

Kuratsu J, Itoyama Y, Uemura S, and Ushio Y (1989) [Regrowth patterns of glioma–cases of glioma regrew away from the original tumor]. *Gan No Rinsho* **35:**1255–1260.

Lagas JS, van Waterschoot RA, Sparidans RW, Wagenaar E, Beijnen JH, and Schinkel AH (2010) Breast cancer resistance protein and P-glycoprotein limit sorafenib brain accumulation. *Mol Cancer Ther* **9:**319–326.

Lagas JS, van Waterschoot RA, van Tilburg VA, Hillebrand MJ, Lankheet N, Rosing H, Beijnen JH, and Schinkel AH (2009) Brain accumulation of dasatinib is restricted by P-glycoprotein (ABCB1) and breast cancer resistance protein (ABCG2) and can be enhanced by elacridar treatment. *Clin Cancer Res* **15:**2344–2351.

Lee G, Babakhanian K, Ramaswamy M, Prat A, Wosik K, and Bendayan R (2007) Expression of the ATP-binding cassette membrane transporter, ABCG2, in human and rodent brain microvessel endothelial and glial cell culture systems. *Pharm Res* **24:**1262–1274.

Leggas M, Panetta JC, Zhuang Y, Schuetz JD, Johnston B, Bai F, Sorrentino B, Zhou S, Houghton PJ, and Stewart CF (2006) Gefitinib modulates the function of multiple ATP-binding cassette transporters in vivo. *Cancer Res* **66:**4802–4807.

Lieberman FS, Fine H, Kuhn J, Lamborn L, Malkin M, Robbins HI, Yung WA, Wen P, and Prados M (2004) NABTC phase I–II study of ZD-1839 for recurrent malignant gliomas and unresectable meningiomas (2004 ASCO Annu Meeting Proceedings). *J Clin Oncol* **22:**1510.

Löscher W and Potschka H (2005) Role of drug efflux transporters in the brain for drug disposition and treatment of brain diseases. *Prog Neurobiol* **76:**22–76.

McKillop D, Partridge EA, Kemp JV, Spence MP, Kendrew J, Barnett S, Wood PG, Giles PB, Patterson AB, Bichat F, et al. (2005) Tumor penetration of gefitinib (Iressa), an epidermal growth factor receptor tyrosine kinase inhibitor. *Mol Cancer Ther* **4:**641–649.

Mellinghoff IK, Cloughesy TF, and Mischel PS (2007) PTEN-mediated resistance to epidermal growth factor receptor kinase inhibitors. *Clin Cancer Res* **13:**378–381.

Mellinghoff IK, Wang MY, Vivanco I, Haas-Kogan DA, Zhu S, Dia EQ, Lu KV, Yoshimoto K, Huang JH, Chute DJ, et al. (2005) Molecular determinants of the response of glioblastomas to EGFR kinase inhibitors. *N Engl J Med* **353:**2012–2024.

Mukasa A, Wykosky J, Ligon KL, Chin L, Cavenee WK, and Furnari F (2010) Mutant EGFR is required for maintenance of glioma growth in vivo, and its ablation leads to escape from receptor dependence. *Proc Natl Acad Sci USA* **107:**2616–2621.

Omuro AM, Faivre S, and Raymond E (2007) Lessons learned in the development of targeted therapy for malignant gliomas. *Mol Cancer Ther* **6:**1909–1919.

Oostendorp RL, Buckle T, Beijnen JH, van Tellingen O, and Schellens JH (2009) The effect of P-gp (Mdr1a/1b), BCRP (Bcrp1) and P-gp/BCRP inhibitors on the in vivo absorption, distribution, metabolism and excretion of imatinib. *Invest New Drugs* **27:**31–40.

Polli JW, Olson KL, Chism JP, John-Williams LS, Yeager RL, Woodard SM, Otto V, Castellino S, and Demby VE (2009) An unexpected synergist role of P-glycoprotein and breast cancer resistance protein on the central nervous system penetration of the tyrosine kinase inhibitor lapatinib (N-{3-chloro-4-[(3-fluorobenzyl)oxy]phenyl}-6-[5-({[2-(methylsulfonyl)ethy l]amino}methyl)-2-furyl]-4-quinazolinamine; GW572016). *Drug Metab Dispos* **37:**439–442.

Rich JN, Reardon DA, Peery T, Dowell JM, Quinn JA, Penne KL, Wikstrand CJ, Van Duyn LB, Dancey JE, McLendon RE, et al. (2004) Phase II trial of gefitinib in recurrent glioblastoma. *J Clin Oncol* **22:**133–142.

Sarkaria JN, Yang L, Grogan PT, Kitange GJ, Carlson BL, Schroeder MA, Galanis E, Giannini C, Wu W, Dinca EB, et al. (2007) Identification of molecular characteristics correlated with glioblastoma sensitivity to EGFR kinase inhibition through use of an intracranial xenograft test panel. *Mol Cancer Ther* **6:**1167–1174.

Silbergeld DL and Chicoine MR (1997) Isolation and characterization of human malignant glioma cells from histologically normal brain. *J Neurosurg* **86:**525–531.

Stommel JM, Kimmelman AC, Ying H, Nabioullin R, Ponugoti AH, Wiedemeyer R, Stegh AH, Bradner JE, Ligon KL, Brennan C, et al. (2007) Coactivation of receptor tyrosine kinases affects the response of tumor cells to targeted therapies. *Science* **318:**287–290.

Wang S, Guo P, Wang X, Zhou Q, and Gallo JM (2008) Preclinical pharmacokinetic/pharmacodynamic models of gefitinib and the design of equivalent dosing regimens in EGFR wild-type and mutant tumor models. *Mol Cancer Ther* **7:**407–417.

Wen PY and Kesari S (2008) Malignant gliomas in adults. *N Engl J Med* **359:**492–507.

Address correspondence to: William F. Elmquist, Department of Pharmaceutics, University of Minnesota, 9-177 Weaver Densford Hall, 308 Harvard Street SE, Minneapolis, MN 55455. E-mail: elmqu011@umn.edu